SCIENTIFIC REPORTS

OPEN

Microscopic model for radiation-induced magnetoresistance oscillations excited by circularly polarized radiation

Received: 21 November 2018
Accepted: 21 June 2019
Published online: 03 July 2019

Jesús Iñarrea[1,2]

We develop a microscopic model to explain the striking result of immunity to the sense of circularly polarized radiation of the photo-excited resistance oscillations in high-mobility 2D electron systems. Our model is based on the radiation-driven electron orbit model, previously developed to explain the photo-induced resistance oscillations and zero resistance states in these systems. According to it, the guiding center of the Landau states when irradiated by circularly polarized radiation performs a circular path driven by radiation. In principle, in an infinite sample, this path is different according to the the sense of circular polarization (left or right). However, the limited size of the sample with the essential role of the edges and the concurrent presence of the Hall electric field tend to quench the displacement of the driven guiding center making nearly equal both trajectories. In the end and in the presence of scattering, the longitudinal irradiated magnetoresistance turns out nearly the same irrespective of the sense of circular radiation.

Microwave-induced resistance oscillations and zero resistance states[1,2] could be revealing a subtle novel form of coupling between radiation and matter. These effects show up in the longitudinal magnetoresistance (R_{xx}) of a high mobility two-dimensional electron system (2DES) when irradiated under a perpendicular magnetic field (B) at low temperatures ($T \sim 1\,K$). Then, unexpected magnetoresistance oscillations rise up superimposed to the well-known longitudinal resistance profile. According to experiments[1,2] the mobility of the sample has to be above $10^6\ cm^2/Vs$ to get to observe them. To date, these oscillations have been obtained with microwave (MW) and terahertz (TH) radiation. When the radiation power (P) is increased, the amplitude of oscillations peaks and valleys increases as well and in the case of valleys, they turn into zero resistance states.

The available experimental evidence proves that these oscillations present some features that can be considered universal: they are periodic in B^{-1}, present a 1/4 cycle phase shift in the oscillations minima[3], are sensitive to temperature (T)[4,5], present a non-linear increase with the radiation power (P) (squared root dependence)[6–16], are immune to the sense of circular polarization in the incident radiation[17], and other intriguing phenomena. Different theoretical models have been presented to try to explain the origin of these effects and their features[18–29]. Yet, after more than a decade of their discovery, they are still under debate and there is no clear consensus about their physical origin.

One of the most intriguing properties of irradiated magnetoresistance oscillations is the role of radiation polarization. According to the available experimental evidence, in the case of linear polarization there is some controversy about the dependence on polarization angle[4,7,17]. Nevertheless, in the case of circular polarization the experimental consensus is clear: the radiation-induced R_{xx} oscillations present immunity against the sense of circularly polarized radiation[17,30]. This is irrespective of radiation power[30] and radiation frequency; this immunity has been detected also when using terahertz frequencies[31]. About the theoretical contributions on polarization immunity, some models conclude that the amplitude of the R_{xx} oscillations changes with the kind of polarization[20] (left-handed or right-handed) showing no immunity. On the other hand there are other theoretical models that offer a physical explanation to this immunity[32,33].

[1]Escuela Politécnica Superior, Universidad Carlos III, 28911 Leganes, Madrid, Spain. [2]Unidad Asociada al Instituto de Ciencia de Materiales, CSIC Cantoblanco, Madrid, 28049, Spain. Correspondence and requests for materials should be addressed to J.I. (email: jinarrea@fis.uc3m.es)

In this article we present a microscopic theoretical approach on the effect of the sense of circularly polarized radiation on irradiated R_{xx} based on a previous theory, developed by the authors: *the radiation-driven electron orbit*[21–25]. This theory is partially based on the displacement model[18] and shares with it that the interplay between charged impurity scattering and radiation is at the heart of the radiation-induced R_{xx} oscillations. However it is different in the way that the radiation-matter interaction is worked out. According to this theory, the irradiated Landau state (LS) is spatially driven by radiation following a classical trajectory given by the solution of the driven classical oscillator. Then, the interaction of the driven-LS with charged impurities ends up giving rise to shorter and longer average advanced distances by the scattered electrons. These shorter and longer distances are reflected on irradiated R_{xx} as valleys and peaks respectively. As a first result of the theory, in an infinite sample the guiding center classical path would be different according to the the sense of circular polarization and thus, we would obtain different results in irradiated R_{xx}. However, the limited size of the 2D sample with the key influence of the edges and the concurrent presence of DC electric fields (driving electric field and the Hall electric field) tend to quench or normalize the displacement of the driven guiding center making nearly equal both trajectories (left and right). In the end and in the presence of charged impurity scattering the radiation-induced oscillations turn out nearly the same irrespective of the sense of circular polarization.

Theoretical Model

We consider a high mobility 2DES in the $x-y$ plane subjected to a static and perpendicular magnetic field, and a DC electric field (driving electric field) parallel to the x direction, E_{dc}. This system is irradiated with circularly polarized radiation, thus, we initially consider for left-handed circular polarization, ($E_x = E_y$), the radiation electric field:

$$\overrightarrow{E}(t) = E_x\,\overrightarrow{x}\,\sin wt - E_y\,\overrightarrow{y}\,\cos wt \tag{1}$$

where E_x and E_y are the electric field amplitudes of the corresponding components of $\overrightarrow{E}(t)$ and $\overrightarrow{x}$ and $\overrightarrow{y}$ are unitary vectors in the x and y directions. w is the frequency of the radiation field. Then, the total hamiltonian H, considering the symmetric gauge for the vector potential of B: $\left(\overrightarrow{A_B} = -\frac{1}{2}\overrightarrow{r} \times \overrightarrow{B}\right)$, reads:

$$\begin{aligned} H &= \frac{P_x^2 + P_y^2}{2m^*} + \frac{w_c}{2}L_z + \frac{1}{2}m^*\left[\frac{w_c}{2}\right]^2[(x - X(0))^2 + y^2] \\ &\quad -\frac{e^2E_{dc}^2}{2m^*\left[\frac{w_c}{2}\right]^2} - [x - X(0)]\,eE_x\cos wt - yeE_y\sin wt \\ &\quad -X(0)eE_0\cos wt \end{aligned} \tag{2}$$

$X(0)$ is the x-coordinate of the LS guiding center: $X(0) = \frac{eE_{dc}}{m^*(w_c/2)^2}$, e is the electron charge, w_c is the cyclotron frequency and L_z is z-component of the electron total angular momentum. The important terms in this hamiltonian are[34,35]: the first is a kinetic term in the x-y plane, the second term is just the energy of the magnetic moment due to the orbital motion in the magnetic field, the third term corresponds to a 2D harmonic oscillator, and finally the term $[-xeE_xcoswt - yeE_ysinwt]$ represents the electromagnetic field. After some algebra[24], the total wave function can be analytically obtained:

$$\Psi(x, y, t) \propto \phi_N[(x - X(0) - x_c(t)), (y - y_c(t)), t] \tag{3}$$

where φ_N are analytical solutions for the Schrödinger equation of a two-dimensional harmonic oscillator (electron under static magnetic field with the symmetric gauge). In polar coordinates the expression for $\varphi_N(r, \theta, t)$[35]:

$$\phi_N = \sqrt{\frac{n!}{2\pi l_B^2 2^{|m|} l_B^{2|m|}(n + |m|)!}}\, r^{|m|}e^{-im\theta}L_n^{|m|}\left(\frac{r^2}{2l_B^2}\right)e^{-\left(\frac{r^2}{4l_B^2}\right)} \tag{4}$$

where n is the radial quantum number, m is the angular momentum quantum number, $L_n^{|m|}$ are the associated Laguerre polynomials and $l_B = \sqrt{\frac{\hbar}{eB}}$ is the effective magnetic length. For the polar coordinates:

$$re^{i\theta} = [x - X(0) - x_c(t)] + i[y - y_c(t)] \tag{5}$$

$x_c(t)$ and $y_c(t)$ are the new coordinates of the guiding center of the radiation-driven LS and are obtained from a system of two coupled classical equations that turn up when solving the previous time dependent Schrodinger equation:

$$\frac{dv_x}{dt} + w_c v_y = \frac{eE_x}{m^*}\sin wt \tag{6}$$

$$\frac{dv_y}{dt} - w_c v_x = -\frac{eE_y}{m^*}\cos wt \tag{7}$$

where v_x and v_y are the components of the guiding center velocity when driven by radiation. Thus, the coordinates of the guiding center are calculated by integrating, $v_x = \frac{dx_c(t)}{dt}$ and $v_y = \frac{dy_c(t)}{dt}$. Then, finally the expressions read,

$$x_c(t) = \frac{eE_x \sin wt}{m^*\sqrt{w^2(w_c - w)^2 + \gamma^4}} + \left[\frac{w_c}{w}\right]\frac{eE_y \sin wt}{m^*\sqrt{w^2(w_c - w)^2 + \gamma^4}} \tag{8}$$

$$y_c(t) = \left[\frac{w_c}{w}\right]\frac{eE_x[1 - \cos wt]}{m^*\sqrt{w^2(w_c - w)^2 + \gamma^4}} + \frac{eE_y[1 - \cos wt]}{m^*\sqrt{w^2(w_c - w)^2 + \gamma^4}} \tag{9}$$

where γ is a damping factor for the electronic interaction with the lattice ions giving rise to acoustic phonons.

The obtained expressions for $x_c(t)$ and $y_c(t)$ correspond, according to our model, to left-handed circularly polarized radiation or cyclotron-resonance active condition (CRA). In our case the right-handed circularly polarized radiation corresponds to the cyclotron-resonance inactive condition (CRI). In the present theoretical model, the left-handed circularly polarized radiation corresponds to the cyclotron-resonance active condition or CRA at positive magnetic field because the radiation polarization direction is the same as the cyclic motion of electrons under the positive magnetic field. In the same way, the cyclotron-resonance inactive condition or CRI corresponds to the right-handed circular radiation because at positive magnetic field the radiation polarization direction is against the cyclic motion of electrons.

In the CRI case the radiation electric field is given by

$$\overrightarrow{E}(t) = E_x\overrightarrow{x} \sin wt + E_y\overrightarrow{y} \cos wt \tag{10}$$

and thus, the system of two coupled equations that are obtained from the Schrodinger equation are given by,

$$\frac{dv_x}{dt} + w_c v_y = \frac{eE_x}{m^*} \sin wt \tag{11}$$

$$\frac{dv_y}{dt} - w_c v_x = \frac{eE_y}{m^*} \cos wt \tag{12}$$

And when solving this system we obtain for the guiding center coordinates for the CRI condition:

$$x_c(t) = \frac{eE_x \sin wt}{m^*\sqrt{w^2(w_c - w)^2 + \gamma^4}} - \left[\frac{w_c}{w}\right]\frac{eE_y \sin wt}{m^*\sqrt{w^2(w_c - w)^2 + \gamma^4}} \tag{13}$$

$$y_c(t) = \left[\frac{w_c}{w}\right]\frac{eE_x[1 - \cos wt]}{m^*\sqrt{w^2(w_c - w)^2 + \gamma^4}} - \frac{eE_y[1 - \cos wt]}{m^*\sqrt{w^2(w_c - w)^2 + \gamma^4}} \tag{14}$$

According to the above expressions of $x_c(t)$ and $y_c(t)$, for both CRA and CRI conditions, the guiding center of LS performs a classical circular trajectory driven by radiation. Both coordinates, $x_c(t)$ and $y_c(t)$, are made up of two contributions, the first one comes from the coupling with radiation along the x-axis and the second one comes from the coupling along the y-axis. This interesting result is the solution of the system of two coupled classical equations where the two coordinates of the guiding center velocity, $v_x(t)$ and $v_y(t)$ appear simultaneously in the two equations of the system. Then, this coupling implies that anything affecting the dynamics of the x-direction (for instance $v_x(t)$ or $v_y(t)$) will affect the dynamics of the y-direction and viceversa.

Now, writing in one equation the two expressions for the two possible modes, active CRA and inactive CRI, for $x_c(t)$, (the one of interest to calculate longitudinal conductivity (σ_{xx}) and R_{xx} we can get to:

$$x_c(t) = \frac{eE_x \sin wt}{m^*\sqrt{w^2(w_c - w)^2 + \gamma^4}} \pm \left[\frac{w_c}{w}\right]\frac{eE_y \sin wt}{m^*\sqrt{w^2(w_c - w)^2 + \gamma^4}} \tag{15}$$

where the $+$ sing corresponds to the CRA mode and the $-$ to the CRI mode. Thus, the second term makes the difference between the two senses of circular radiation. The bigger this term, the bigger will be difference in irradiated R_{xx} between CRA and CRI; the experimentally observed circularly polarized radiation immunity of irradiated R_{xx} will depend, according to our theory, on this term.

The result of Eq. 15 corresponds to a 2D infinite sample, but in a real case the limited size of the sample, with the existence of edges in x and y directions, and the concurrence of the driving DC-electric field (responsible of the current in the x-direction) and the Hall electric field, will necessary alter the displacement of the guiding center. Besides, another important point that stems from the radiation-driven electron orbits model, can affect also the dynamics of the driven-LS guiding center in conjunction with the existence of sample edges: the spatial shift of the whole 2DES driven by radiation with respect to the fixed positive background of the lattice ions. This effect gives rise to the appearance of areas of opposite and alternate charge on either end of the sample creating electrostatic repulsion and attraction interactions (see Fig. 1). In other words, an alternate electric field inside the 2D sample that tends to go against the radiation-driven displacement of the LS guiding center. All of the above sample edge-related effects make the guiding center to slow down in its classical trajectory. The general outcome

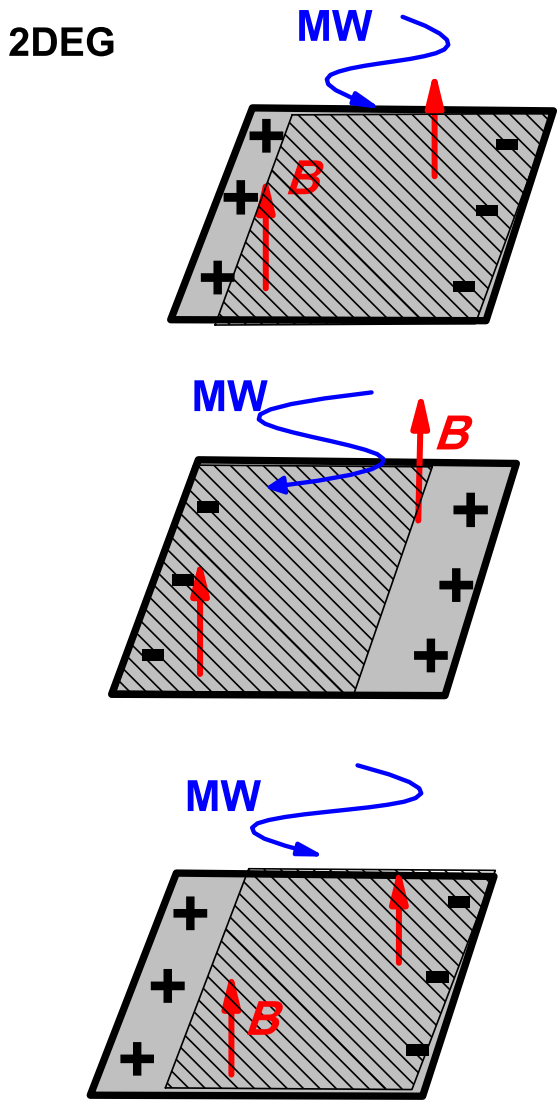

Figure 1. Schematic diagrams showing the dynamics of a two-dimensional electron system driven by radiation. The figures shown here represent only the spatial effect of radiation on the 2DES. The latter is being spatially driven when illuminated by microwave radiation. The radiation-driven oscillating 2D electron gas together with the existence of sample edges produce an alternating change in the position of the charged stripes at every end of the sample: an alternate electric field inside the 2D sample that goes against the radiation-driven trajectory of the LS guiding center. This effect slows down the motion of the driven-2DES.

is a built-in quenching or damping effect on the radiation-driven motion of the guiding center making nearly equal or very similar the coordinate $x_c(t)$ of both CRA and CRI modes. To reflect this we propose at this point a phenomenological model where we introduce two damping factors affecting the amplitudes E_x and E_y and the corresponding delays in the sine terms (similar to the case of classical damped oscillators). Now and in the most general approach, we consider that this damping can be of different intensity for the x and y contribution to $x_c(t)$. For instance, we can physically justify this asymmetry in the damping, by the higher intensity of the Hall field compared to the DC-driving field; the point is that the motion along the y-direction, parallel to the Hall field, could be more hampered by the presence of this field than the one in the x-direction.

Thus, the total expression of $x_c(t)$ would be given by

$$x_c(t) = \frac{e^{-\gamma_x t} eE_x \sin(wt + \varphi_x)}{m^* \sqrt{w^2(w_c - w)^2 + \gamma^4}} \pm \left[\frac{w_c}{w}\right] \frac{e^{-\gamma_y t} eE_y \sin(wt + \varphi_y)}{m^* \sqrt{w^2(w_c - w)^2 + \gamma^4}} \tag{16}$$

where γ_x, γ_y and damping terms and φ_x and φ_y are phase differences. All of them are phenomenologically introduced according to our model. We can simplify the latter equation summing up the two terms considering that for left-handed circular radiation, $E_x = E_y = E_0$:

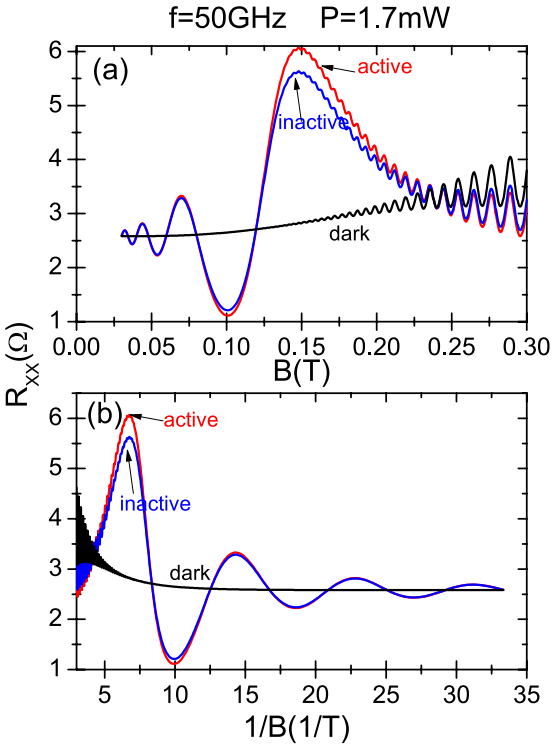

Figure 2. Calculated linear magnetoresistance vs magnetic field (upper panel) and vs the inverse of the magnetic field (lower panel) under circularly polarized radiation for CRA and CRI conditions. The radiation frequency is $f = 50$ GHz and temperature $T = 1$ K. The edge-damping $\gamma_y = 0.2 \times 10^{10} s^{-1}$ and the phase difference, $\varphi = \pi/3$. The dark case is displayed. For the irradiated curves, we observe that the radiation-induced oscillations are periodic in B^{-1} and the minima 1/4-cycle shifted. It is clearly observed that the irradiated magnetoresistivity response for the CRA and CRI conditions is nearly the same over the whole range of magnetic field.

$$x_c(t) = \left[\frac{\sqrt{e^{-2\gamma_x t}w^2 + e^{-2\gamma_y t}w_c^2 \pm 2ww_c e^{-(\gamma_x+\gamma_y)t}\cos\varphi}}{w}\right]\frac{eE_0\sin(wt+\alpha)}{m^*\sqrt{w^2(w_c-w)^2+\gamma^4}} \tag{17}$$

If now and according to our phenomenological model, $e^{-\gamma_y t} = ae^{-\gamma_x t}$, where $a < 1$ assuming that the sample edge damping is more intense in the y-direction than in the x-direction, then we can finally write for $x_c(t)$,

$$x_c(t) = \left[\frac{\sqrt{w^2 + a^2w_c^2 \pm 2aww_c\cos\varphi}}{w}\right]\frac{eE_0e^{-\gamma_x t}\sin(wt+\alpha)}{m^*\sqrt{w^2(w_c-w)^2+\gamma^4}} \tag{18}$$

$$= A^*e^{-\gamma_x t}\sin(wt+\alpha) \tag{19}$$

where the amplitude A^* is given by:

$$A^* = \left[\frac{\sqrt{w^2 + a^2w_c^2 \pm 2aww_c\cos\varphi}}{w}\right]\frac{eE_0}{m^*\sqrt{w^2(w_c-w)^2+\gamma^4}} \tag{20}$$

where $\varphi = \varphi_y - \varphi_x$. The phase difference α can be left out with the appropriate time shift (all driven-LS are oscillating in phase). And the total electronic orbit center coordinate in the x-direction, $X(t)$, changes according to our model by[29]

$$\begin{aligned} X(t) &= X(0) + x_c(t) \\ &= X(0) + A^*e^{-\gamma_x t}\sin wt \end{aligned} \tag{21}$$

Following the radiation-driven electron orbit model we can obtain the advanced distance by the electron due to charged impurity scattering when jumping between irradiated LS[29]:

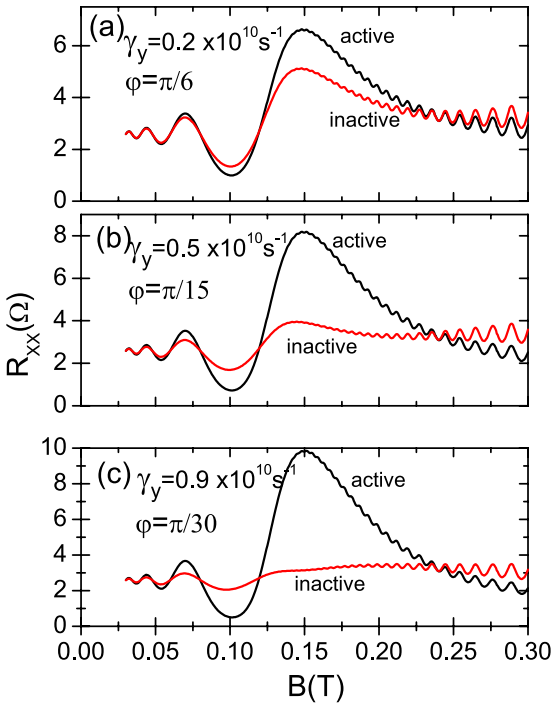

Figure 3. Calculated magnetoresistance under radiation vs magnetic field in three different panels for increasing values of the edge-damping γ_y and decreasing of the phase difference φ. In panel (a) $\gamma_y = 0.2 \times 10^{10} s^{-1}$ and $\varphi = \pi/6$, in panel (b) $\gamma_y = 0.5 \times 10^{10} s^{-1}$ and $\varphi = \pi/15$, and in panel (c) $\gamma_y = 0.9 \times 10^{10} s^{-1}$ and $\varphi = \pi/30$. We observe that as γ_y gets bigger and closer to γ_x, and the phase difference φ gets smaller, the traces of both CRA and CRI increasingly diverge. Remarkably, the divergence of both conditions gets bigger as the magnetic field increases for each panel irrespective of the value of γ_y and φ. T = 1 K.

$$\begin{aligned} \Delta X &= \Delta X(0) - A^* e^{-\gamma_x \tau} \sin(w\tau) \\ &= \Delta X(0) - A^* e^{-\gamma_x \frac{2\pi}{w_c}} \sin\left(2\pi \frac{w}{w_c}\right) \end{aligned} \tag{22}$$

where $\Delta X(0)$ is the shift of the guiding center coordinate for the eigenstates involved in the scattering event when there is no light. According to the radiation-driven electron orbit model, the time $\tau = \frac{2\pi}{w_c}$ is the *flight time* or the time it takes the electron to jump from a Landau state to another one due to scattering.

Applying these last results to a Boltzmann transport model[34,36–38], where σ_{xx} is given by:

$$\sigma_{xx} = e^2 \int_0^\infty dE \rho_i(E) [\Delta X]^2 W_I \left(-\frac{df(E)}{dE}\right) \tag{23}$$

being E the energy, $\rho_i(E)$ the density of initial states, $f(E)$ the electron distribution function and W_I the charged impurity scattering rate, we can get to a final expression for σ_{xx}[29,34,36–38],

$$\sigma_{xx} \propto \left[\Delta X^0 - A^* e^{-\gamma_x \frac{2\pi}{w_c}} \sin\left(2\pi \frac{w}{w_c}\right)\right]^2 \left[1 + e^{\frac{-\pi\Gamma}{\hbar w_c}} \frac{X_S}{\sinh X_S} \cos\left(2\pi \frac{E_F}{\hbar w_c}\right)\right] \tag{24}$$

where Γ is the LS width, E_F stands for the Fermi energy and $X_S = \frac{2\pi^2 k_B T}{\hbar w_c}$, k_B being the Boltzmann constant. To obtain R_{xx} we use the relation $R_{xx} = \frac{\sigma_{xx}}{\sigma_{xx}^2 + \sigma_{xy}^2} \simeq \frac{\sigma_{xx}}{\sigma_{xy}^2}$, where $\sigma_{xy} \simeq \frac{n_i e}{B}$ and $\sigma_{xx} \ll \sigma_{xy}$, n_i being the 2D electron density.

Within a more general approach we could extend to the Hall resistance, R_{xy}, what we have applied to R_{xx}. According to the model the charge strips would be changing with radiation in x and y direction and this should affect the Hall voltage and the Hall resistance. Thus, a possible effect on the Hall resistance would be an alternate voltage to be added to the total Hall voltage. The value of the Hall electric field is high and maybe the radiation effect on it could be very small. This would depend mainly of the radiation power.

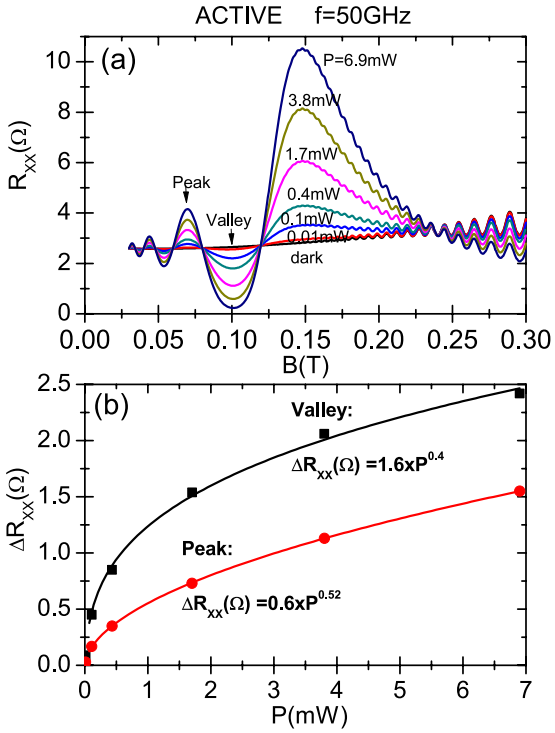

Figure 4. Dependence on radiation power P of the calculated magnetoresistivity under circularly polarized light for the CRA condition. The edge-damping $\gamma_y = 0.2 \times 10^{10} s^{-1}$ and the phase difference, $\varphi = \pi/3$. In panel (a) irradiated R_{xx} as a function of B, for different radiation intensities starting from dark and for a radiation frequency of $f = 50$ GHz. We observed that the R_{xx} oscillations amplitudes increase with an increasing power. In panel (b) $\Delta R_{xx} = R_{xx}(light) - R_{xx}(dark)$ versus P for B corresponding to the peak and valley labels of panel (a). For both sets of R_{xx} values we obtain a square root dependence as shown in the corresponding fits where the exponent of P is around 0.5. T = 1 K.

Results and Discussion

All the calculated curves presented in this section are based on Eq. 24 and on the tensor relation between R_{xx} and σ_{xx} (see above). In Fig. 2 we exhibit radiation-induced R_{xx} oscillations vs magnetic field under circularly polarized radiation for CRA and CRI modes. The radiation frequency is $f = 50$ GHz and temperature $T = 1$ K. The dark case is also presented. For the irradiated traces, we observe that the radiation-induced oscillations are periodic in B^{-1} and the minima are 1/4-cycle shifted. Interestingly enough, we observe that the irradiated magnetoresistivity response for the CRA and CRI conditions is nearly the same over the whole range of magnetic field. There seems to be a small difference around cyclotron resonance. The general calculated result is in qualitatively agreement with experiment[17,30]. In our simulations we have used experimental values for radiation power and frequency, temperature, electron density, type of sample, etc.[30]. Thus, using these experimental values and in order to achieve circular polarization immunity, we have obtained phenomenological values for the edge-damping $\gamma_x \simeq 10^{10}\ s^{-1}$, $\gamma_y \simeq 0.1 \times 10^{10}\ s^{-1}$, and for the phase difference $\varphi \simeq \pi/3$. We can consider these values as the threshold between immunity and non-immunity scenarios according to experimental parameters[17,30]. In platforms with a lesser influence of the sample edges, we would obtain a clear difference between irradiated R_{xx} for CRA and CRI modes. This is what we display in Fig. 3, where it is exhibited calculated magnetoresistance under radiation vs magnetic field in three different panels for three different values of the edge-damping γ_y and φ and same value of γ_x. In panel (a) $\gamma_y = 0.2 \times 10^{10} s^{-1}$ and $\varphi = \pi/6$, in panel (b) $\gamma_y = 0.5 \times 10^{10} s^{-1}$ and $\varphi = \pi/15$, and in panel (c) $\gamma_y = 0.9 \times 10^{10} s^{-1}$ and $\varphi = \pi/30$. It is clear that as γ_y gets bigger and closer to γ_x, and the phase difference φ gets smaller, the traces of both CRA and CRI increasingly diverge: the CRA trace increases and the CRI decreases. And in the same way, this divergence gets bigger as the magnetic field increases. This latter behavior is qualitatively similar for the three panels irrespective of the value of γ_y and φ.

In Fig. 4 we present the dependence of calculated irradiated R_{xx} on P for the CRA condition. In panel (a) we display R_{xx} vs magnetic field for a radiation frequency of 50 GHz whereas the power ranges from 0.01 mW to 6.9 mW. In between we also exhibit traces of 0.1, 0.4, 1.7 and 3.8 mW. The dark case is also presented. The temperature used is $T = 1$ K. The sample edge damping parameters correspond to the ones of Fig. 2, i.e., a scenario of circular polarization immunity. We observe, as expected, that magnetoresistance oscillations increase their amplitudes as P increases from dark. In panel (b) we exhibit, for the same radiation frequency $\Delta R_{xx} = R_{xx}(light) - R_{xx}(dark)$ versus P for the magnetic fields labelled in panel (a) with peak and valley. The power dependence of the oscillatory R_{xx} clearly indicates a non-linear behavior. We want to check out the previously obtained sublinear power law for the dependence of irradiated R_{xx} on P. In this way we obtain for both sets of R_{xx} values, according to the calculated fits, an approximately square root dependence on P. For the valley trace we

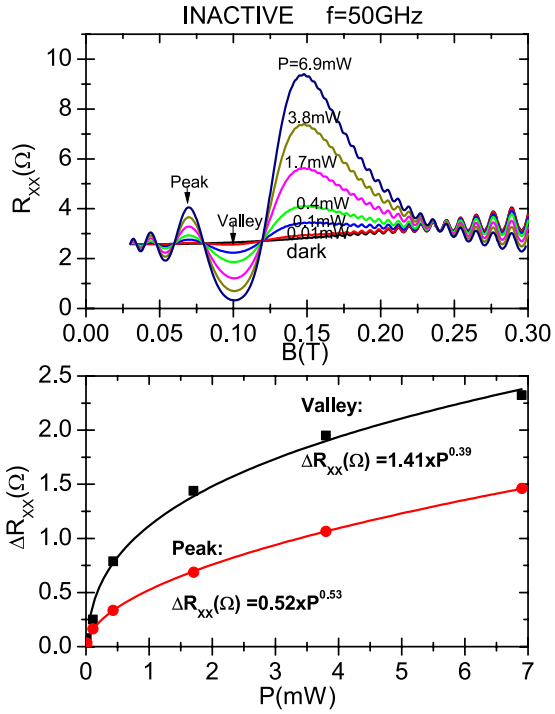

Figure 5. Same as in Fig. 4 but for the CRI condition. The edge-damping $\gamma_y = 0.2 \times 10^{10}\, s^{-1}$ and the phase difference, $\varphi = \pi/6$. In panel (a) traces of irradiated R_{xx} vs B for the same radiation powers as in Fig. 4. All of them are nearly the same as the ones of CRA condition proving circular polarization immunity. In panel (b) $\Delta R_{xx} = R_{xx}(light) - R_{xx}(dark)$ versus P for the magnetic fields labelled in panel (a) with peak and valley. We obtain for both sets of R_{xx} values calculated fits showing approximately square root dependence on P. T = 1 K.

obtain a fit given by $\Delta R_{xx} = 1.6 \times P^{0.4}$ and for the peak $\Delta R_{xx} = 0.6 \times P^{0.52}$; for both cases the exponent is around 0.5 that implies a square root dependence. We can theoretically explain these results according to the radiation-driven electron orbit model: in the expression of σ_{xx} and then in R_{xx}, P only shows up in the numerator of the amplitude A^* as $\sqrt{P} \propto E_0$, the radiation electric field. Thus, on the one hand, P does not affect the phase of R_{xx} oscillations that remains constant as P changes, and on the other hand $R_{xx} \propto \sqrt{P}$, giving rise to the sublinear (square root) power law for the dependence of R_{xx} on P.

In Fig. 5 we present the same as in Fig. 4 but for the CRI condition. In panel (a) we show traces of irradiated R_{xx} vs magnetic field for the same radiation powers as Fig. 4. All of them are nearly the same as the ones of CRA condition proving circular polarization immunity except for a region of magnetic fields around the cyclotron resonance. In panel (b) we exhibit $\Delta R_{xx} = R_{xx}(light) - R_{xx}(dark)$ versus P for the magnetic fields labelled in panel (a) with peak and valley. We obtain for both sets of R_{xx} values calculated fits that show approximately a square root dependence on P too. For the valley trace we obtain a fit given by $\Delta R_{xx} = 1.41 \times P^{0.39}$ and for the peak $\Delta R_{xx} = 0.52 \times P^{0.53}$. Thus, as in the active condition, we obtain exponents for P around 0.5. This proves a square root dependence as predicted by the radiation-driven electron orbit model.

Another remarkable result that is obtained from Figs 4 and 5 is that the immunity of radiation-induced magnetoresistance oscillations to the orientation of the circular polarization holds independently of radiation power. This an expected result according to Eqs 20 and 24 of the model. According to them, it is clear that the power variation would affect in the same way both circular polarization conditions, CRA and CRI.

References

1. Mani, R. G. *et al*. Zero-resistance states induced by electromagnetic-wave excitation in GaAs/AlGaAs heterostructures. *Nature* **420**, 646 (2002).
2. Zudov, M. A., Lu, R. R., Pfeiffer, N. & West, K. W. Evidence for a New Dissipationless Effect in 2D Electronic Transport. *Phys. Rev. Lett.* **90**, 046807 (2003).
3. Mani, R. G. *et al*. Demonstration of a 1/4-Cycle Phase Shift in the Radiation-Induced Oscillatory Magnetoresistance in GaAs/AlGaAs Devices. *Phys. Rev. Lett.* **92**, 146801 (2004).
4. Mani, R. G., Gerl, C., Schmult, S., Wegscheider, W. & Umansky, V. Nonlinear growth in the amplitude of radiation-induced magnetoresistance oscillations. *Phys. Rev. B* **81**, 125320 (2010).
5. Iñarrea, J. & Platero, G. Temperature effects on microwave-induced resistivity oscillations and zero-resistance states in two-dimensional electron systems. *Phys. Rev. B* **72**, 193414 (2005).
6. Jesus Inarrea, R. G. M. & Wegscheider, W. Sublinear radiation power dependence of photoexcited resistance oscillations in two-dimensional electron systems. *Phys. Rev.* **82**, 205321 (2010).
7. Mani, R. G., Ramanayaka, A. N. & Wegscheider, W. Observation of linear-polarization-sensitivity in the microwave-radiation-induced magnetoresistance oscillations. *Phys. Rev. B.* **84**, 085308 (2011).
8. Ramanayaka, A. N., Mani, R. G., Inarrea, J. & Wegscheider, W. Effect of rotation of the polarization of linearly polarized microwaves on the radiation-induced magnetoresistance oscillations. *Phys. Rev. B.* **85**, 205315 (2012).

9. Ye, T., Inarrea, J., Wegscheider, W. & Mani, R. G. Linear polarization study of microwave-radiation-induced magnetoresistance oscillations: Comparison of power dependence to theory. *Phys. Rev. B.* **94**, 035305 (2016).
10. Inarrea, J. Influence of linearly polarized radiation on magnetoresistance in irradiated two-dimensional electron systems. *Appl. Phys Lett.* **100**, 242103 (2012).
11. Mani, R. G. *et al*. Radiation-induced oscillatory Hall effect in high-mobility GaAs/AlxGa1-xAs devices. *Phys. Rev. B* **69**, 161306(R) (2004).
12. Mani, R. G. *et al*. Radiation-induced zero-resistance states in GaAsAlGaAs heterostructures: Voltage-current characteristics and intensity dependence at the resistance minima. *Phys. Rev. B* **70**, 155310 (2004).
13. Mani, R. G. & Kriisa, A. Magneto-transport characteristics of a 2D electron system driven to negative magneto-conductivity by microwave photoexcitation. *Sci. Rep.* **3**, 3478 (2013).
14. Samaraweera, R. L. *et al*. Mutual influence between currentinduced giant magnetoresistance and radiation-induced magnetoresistance oscillations in the GaAs/AlGaAs 2DES. *Sci. Rep.* **7**, 5074 (2017).
15. Wang, Z., Samaraweera, R. L., Reichl, C., Wegscheider, W. & Mani, R. G. Tunable electron heating induced giant magnetoresistance in the high mobility GaAs/AlGaAs 2D electron system. *Sci. Rep.* **6**, 38516 (2016).
16. Gunawardana, B. *et al*. Millimeter wave radiation-induced magnetoresistance oscillations in the high quality GaAs/AlGaAs 2D electron system under bichromatic excitation. *Phys. Rev. B* **95**, 195304 (2017).
17. Smet, J. H. *et al*. Circular-polarization-dependent study of the microwave photoconductivity in a two-dimensional electron system. *Phys. Rev. Lett.* **95**, 116804 (2005).
18. Durst, A. C., Sachdev, S., Read, N. & Girvin, S. M. Radiation-Induced Magnetoresistance Oscillations in a 2D Electron Gas. *Phys. Rev. Lett.* **91**, 086803 (2003).
19. Vavilov, M. G. *et al*. Compressibility of a two-dimensional electron gas under microwave radiation. *Phys. Rev. B* **70**, 161306 (2004).
20. Lei, X. L. & Liu, S. Y. Radiation-Induced Magnetoresistance Oscillation in a Two-Dimensional Electron Gas in Faraday Geometry. *Phys. Rev. Lett.* **91**, 226805 (2003).
21. Iñarrea, J. & Platero, G. Theoretical Approach to Microwave-Radiation-Induced Zero-Resistance States in 2D Electron Systems. *Phys. Rev. Lett.* **94**, 016806 (2005).
22. Inarrea, J. Evidence of radiation-driven Landau states in 2D electron systems: Magnetoresistance oscillations phase shift. *Euro. Phys Lett.* **113**, 57004 (2016).
23. Inarrea, J. & Platero, G. From zero resistance states to absolute negative conductivity in microwave irradiated two-dimensional electron systems. *Appl. Phys. Lett.* **89**, 052109 (2006).
24. Inarrea, J. & Platero, G. Microwave-induced resistance oscillations versus magnetoabsorption in two-dimensional electron systems: role of temperature. *Nanotechnology* **21**, 315401 (2010).
25. Inarrea, J. & Platero, G. Microwave-induced resistance oscillations and zero-resistance states in two-dimensional electron systems with two occupied subbands. *Phys. Rev. B* **84**, 075313 (2011).
26. Inarrea, J. & Platero, G. Radiation-induced resistance oscillations in a 2D hole gas: a demonstration of a universal effect. *J. Phys.:Condens. Matter* **69**, 415801 (2015).
27. Inarrea, J. The two dimensional electron system as a nanoantenna in the microwave and terahertz bands. *Appl. Phys. Lett* **99**, 232115 (2011).
28. Inarrea, J. & Platero, G. Driving Weiss oscillations to zero resistance states by microwave Radiation. *Appl. Phys Lett* **93**, 062104 (2008).
29. Inarrea, J. Radiation-induced resistance oscillations in 2D electron systems with strong Rashba coupling. *Sci. Rep* **7**, 13573 (2017).
30. Ye, T., Liu, H.-C., Wang, Z., Wegscheider, W. & Ramesh, G. M. Comparative study of microwave radiation-induced magnetoresistive oscillations induced by circularly- and linearlypolarized photo-excitation. *Sci. Rep.* **5**, 14880 (2015).
31. Herrmann, T. *et al*. Analog of microwave-induced resistance oscillations induced in GaAs heterostructures by terahertz radiation. *Phys. Rev. B.* **94**, 081301 (2016).
32. Inarrea, J. & Platero, G. Polarization immunity of magnetoresistivity response under microwave radiation. *Phys. Rev. B* **76**, 073311 (2007).
33. Shenshen, W. & Tai-Kai, N. Circular-polarization independence of microwave-induced resistance oscillations and the zero-resistance state. *Phys. Rev. B* **77**, 165324 (2008).
34. Miura, N. Physics of Semiconductors in High Magnetic Fields. 1st. ed. Oxford University Press. Oxford (2008).
35. Friedrich, H. Theoretical Atomic Physics. 4th ed. Springer. Munchen, Germany (2017).
36. Ridley, B. K. Quantum Processes in Semiconductors, 4th ed. Oxford University Press (1993).
37. Ando, T., Fowler, A. & Stern, F. Electronic properties of two-dimensional systems. *Rev. Mod. Phys.* **54**, 437 (1982).
38. Askerov, B. M. Electron trnasport phenomena in semiconductors. World Scientific, Singapore (1994).

Acknowledgements

This work is supported by the MINECO (Spain) un- der grant MAT2017-86717-P and ITN Grant 234970 (EU). GRUPO DE MATEMATICAS APLICADAS A LA MATERIA CONDENSADA, (UC3M), Unidad Asociada al CSIC.

Additional Information

Competing Interests: The author declares no competing interests.

Publisher's note: Springer Nature remains neutral with regard to jurisdictional claims in published maps and institutional affiliations.